Light-Responsive Threadlike Micelles as Drag Reducing Fluids with Enhanced Heat-Transfer Capabilities

Haifeng Shi,[†] Yi Wang,[⊥] Bo Fang,[†,⊗] Yeshayahu Talmon,[‡] Wu Ge,[§] Srinivasa R. Raghavan,[∥] and Jacques L. Zakin*,[†]

[†]Department of Chemical and Biomolecular Engineering, Ohio State University, 140 West 19th Avenue, Columbus, Ohio 43210, United States

[‡]Department of Chemical Engineering, Technion—Israel Institute of Technology, Haifa 32000, Israel
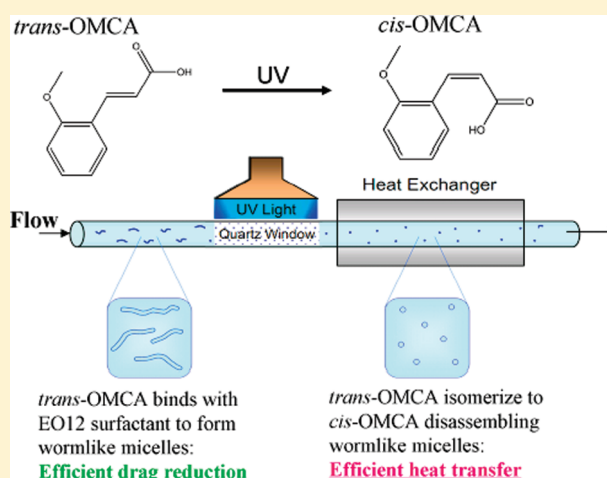
[§]Kraft Foods Global Research, Glenview, Illinois 60025, United States

[∥]Department of Chemical and Biomolecular Engineering, University of Maryland, College Park, Maryland 20742, United States

[⊥]Beijing Key Laboratory of Urban Oil and Gas Distribution Technology, China University of Petroleum-Beijing, Beijing 102249, China

S *Supporting Information*

ABSTRACT: Drag-reducing (DR) surfactant fluids based on threadlike micelles are known to suffer from poor heat-transfer capabilities. Accordingly, the use of these fluids is limited to recirculating systems in which heat exchange is not important. Here, we show for the first time that light-responsive threadlike micelles can offer a potential solution to the above problem. The fluids studied here are composed of the cationic surfactant Ethoquad O/12 PG (EO12) and the sodium salt of *trans-ortho*-methoxycinnamic acid (OMCA). Initially, these fluids contain numerous threadlike micelles and, in turn, are strongly viscoelastic and effective at reducing drag (up to 75% DR). Upon exposure to UV light, OMCA is photoisomerized from trans to cis. This causes the micelles to shorten considerably, as confirmed by cryo-transmission electron microscopy (cryo-TEM). Because of the absence of long micelles, the UV-irradiated fluid shows lower viscoelasticity and much lower DR properties; however, its heat-transfer properties are considerably superior to the initial fluid. Thus, our study

highlights the potential of switching off the DR (and in turn enhancing heat-transfer) at the inlet of a heat exchanger in a recirculating system. While the fluids studied here are not photoreversible, an extension of the above concept would be to subsequently switch on the DR again at the exit of the heat exchanger, thus ensuring an ideal combination of DR and heat-transfer properties.

1. INTRODUCTION

In 1931, Forrest and Grierson[1] first observed a reduced pressure loss of turbulent flow when they studied wood-pulp fiber suspensions in water. This reduction in pressure loss is termed turbulent drag reduction (DR), and it is beneficial in fluid transport because it translates into lower energy requirements for pumping the fluid. Since then, many additives including high-molecular-weight linear polymers and surfactants that form threadlike micelles have been studied as DR agents.[2] Maximum DR asymptotes have been established for polymer solutions[3] and micellar solutions.[4] The maximum DR achievable with threadlike micelles is greater than that with high polymers. Another advantage of threadlike micelles over high polymers is that they can reassemble after being broken up by high shear-stresses.

Threadlike micelles are formed in water by many cationic surfactants in the presence of certain counterions.[5,6] The presence of these micelles can be inferred from the viscoelastic properties of the solutions. Threadlike micelles in solution can be directly observed by the cryo-transmission electron microscopy (cryo-TEM).[7-15] It is generally believed that threadlike micelles must be present for surfactant solutions to be drag reducing.[16-19] Qi[20] proposed two mechanisms to explain how threadlike micelles reduce drag. First, the long micellar chains may help to damp small turbulent eddies and reduce the dissipation of turbulent energy. Second, the alignment of threadlike micelles along the flow may cause anisotropic resistance to turbulent vortices, resulting in suppressed flow fluctuations in the direction

normal to the flow. The latter has been confirmed by Gyr and Buhler[21] and Tamano et al.[22]

In cationic surfactant systems, organic counterions promote the growth of threadlike micelles.[19] In particular, certain counterions with hydrophobic aromatic groups bind strongly to cationic micelles with their aromatic rings buried into the hydrophobic core of the micelles.[23] Such binding of counterions neutralizes the charge on the surfactant headgroups and thereby decreases the effective area per headgroup, which in turn promotes the growth of threadlike micelles at the expense of spherical ones.[24] For optimal binding to micelles, the counterion should be able to orient its hydrophilic and hydrophobic parts in their favored environments.[8,15,24−26] If the molecular configuration of the counterion is altered by an external stimulus (e.g., light), adsorbed counterions could desorb, and vice versa. This aspect is used in the design of light-responsive micelles (see below).

Threadlike micellar solutions are considered for use in recirculating systems such as for district heating and cooling (DHC), where their DR properties help to save pumping energy.[19] However, the utility of these solutions in DHC is limited because the same solutions also have reduced heat-transfer ability compared to pure water.[27−33] Although the causes of reduced heat-transfer are complex, they may be related to two characteristics of DR solutions. First, the viscous sublayer in a viscoelastic fluid can be considerably thicker than in a Newtonian fluid.[34] This thickened viscous sublayer provides greater thermal resistance between the wall of a heat exchanger and the bulk flow of a DR fluid and thus decreases heat transfer from the fluid to the wall.[20] In addition, threadlike micelles greatly suppress the velocity fluctuations in the radial direction in turbulent flow,[21,35] which reduces heat transfer in the radial direction.[20] Also in the region near the wall, reduced wall-normal turbulence intensity,[22,36] disappearance of strong vorticity fluctuation,[37] and reduced strength and frequency of turbulent bursts[38] have been observed in drag-reducing surfactant solutions. In short, the properties that allow threadlike micelles to reduce turbulent drag also cause them to negatively impact heat transfer.

Various in-flow devices have been studied to temporarily enhance the heat-transfer properties of a DR fluid, either by destroying threadlike micelles or disturbing the flow. These include fluted-tube heat exchangers,[39] wire meshes,[40] static mixers,[41] metal grids,[42] helical pipes,[43] low-profile vortex generators,[44] and impinging jets.[45] However, each of these devices creates additional resistance to the flow, causing a significant penalty in terms of energy-loss. One alternative to such in-flow devices is the use of ultrasonic energy to enhance heat transfer externally;[46] however, this method was also not economical in energy cost.

In this paper, we describe a new approach for enhancing the heat-transfer properties of drag-reducing micellar solutions. This approach involves the use of light-responsive threadlike micelles. Threadlike micelles can be made responsive to light by incorporating photosensitive groups in the structure of the counterions[47−49] or the surfactants.[50−53] However, these custom-made surfactants are expensive and difficult to synthesize; hence, they are not viable candidates for DR systems. Recently, a range of light-responsive micellar solutions using only inexpensive, commercially available components have been developed by Raghavan and co-workers.[54,55] These solutions showed significant changes in their rheological properties upon exposure to UV light; they were hence termed photorheological (PR) fluids. Of particular interest here is the system described by Ketner et al.,[54] a mixture of the cationic surfactant, cetyl trimethylammonium bromide (CTAB) and the photosensitive counterion *trans-ortho*-methoxycinnamic acid (*trans*-OMCA).

Mixtures of CTAB and OMCA were viscoelastic; and long cylindrical microstructures were indicated by small-angle neutron scattering. When exposed to UV light, *trans*-OMCA was photoisomerized to its cis form and, in turn, the micelles became much shorter. These changes occurred because the binding affinity of *trans*-OMCA to CTAB micelles was much stronger than that of *cis*-OMCA.

In the present study, we create drag-reducing fluids by combining OMCA with the cationic surfactant, oleyl bis(2-hydroxyethyl)methyl ammonium chloride (Ethoquad O/12 PG or EO12). We show that EO12/OMCA solutions contain threadlike micelles and are thus effective at DR, while their heat-transfer properties are poor. When the solutions are exposed to UV light (converting OMCA from trans to cis), the micelles get shortened, as shown here by cryo-TEM. In turn, the DR properties are reduced, but the heat transfer is substantially improved. Thus, our study suggests the possibility of switching a fluid between states conducive to effective drag-reduction and effective heat-transfer. We should point out that we have not yet succeeded in reversing the isomerization to restore *trans*-OMCA and regain effective drag reduction. Our goal is to switch off and on repeatedly between the two above states. Nevertheless, we selected this counterion due to its low-cost and availability to initiate our study on photoswitchable systems. Studies with photoreversible counterions will be explored in the future. Eventually, we anticipate that switchable fluids exhibiting a combination of good drag reduction and heat transfer properties will prove attractive for use in recirculating DHC systems. A scheme for application of switchable fluids is proposed (Supporting Information, Scheme S1).

2. EXPERIMENTAL SECTION

2.1. Recirculation System. Our recirculation system for drag reduction and heat-transfer experiments has a total length of about 25 m and can hold up to 16 L of liquid. Pressure drop and heat transfer were measured at controlled temperature and flow rates. All the thermocouples, pressure transmitters, and flow meters are connected to the data acquisition system detailed by Ge.[56] (See Supporting Information for details of the recirculation system and tube-in-tube heat exchanger (Scheme S2), and experimental procedure.)

2.2. Materials and Sample Preparation. Ethoquad O/12 PG (donated by Akzo Nobel) is a mixture of oleyl bis(2-hydroxyethyl)methyl ammonium chlorides (75 wt %) and propylene glycol (25 wt %). OMCA in its native trans form (purity >99%) as well as *cis*-OMCA (purity >98%) were purchased from TCI America.

Surfactant/counterion solutions for drag reduction and heat transfer experiments were prepared by continuously stirring the solution in a bucket for 8 h at room temperature with a high shear disperser (Janke & Hunkel IKA Ultra-Turrax SD-45). Sodium hydroxide was used to maintain the pH of the solutions between 8 and 10. The solutions were then left to rest overnight at room temperature. Solutions in smaller quantities were stirred with magnetic stirrers overnight before rheological and other analytical measurements. To minimize exposure to any light, all the solutions were well covered during preparation and storage.

2.3. Drag Reduction and Heat Transfer Measurement. To estimate the extent of DR, pressure drops were measured at different flow rates at a steady state at fixed temperatures. The friction factor, *f*, was calculated according to eq 1:

$$f = \frac{\Delta P D}{2\rho L V^2} \tag{1}$$

where ΔP the pressure drop across the test section, D the inner diameter of the pipe, ρ the density of the solution, L the length of the test section, and V the mean flow velocity. Since ρ was essentially identical for the solutions and the solvent (water), the extent of DR (relative to water) could be calculated
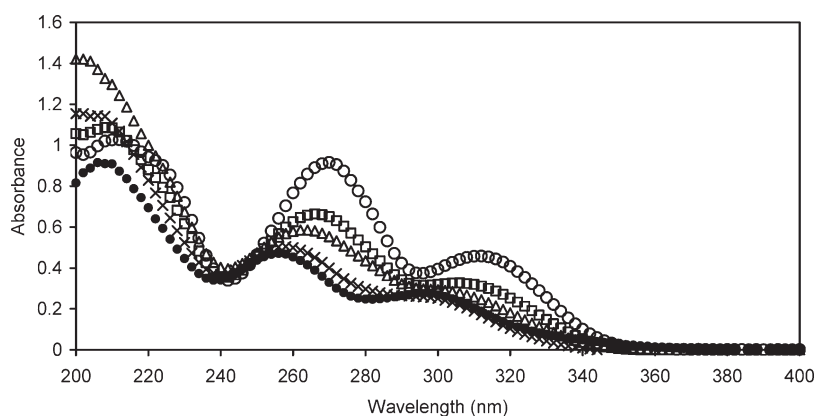
Figure 1. UV−vis spectra for 0.04 mM EO12 + 0.05 mM *trans*-OMCA after different durations of UV irradiation and also for 0.05 mM *cis*-OMCA. ○, before UV; □, UV for 1 min; △, UV for 2 min; ×, UV for 4 min; ●, *cis*-OMCA.

according to eq 2:

$$\% \ DR = \frac{f_{water} - f}{f_{water}} \times 100\% \qquad (2)$$

where % DR is percent drag reduction and f_{water} is the friction factor of water. For direct comparison, f_{water} and f were taken at the same solvent Reynolds number, Re, (i.e., using the viscosity of water). Re is $DV\rho/\eta$, where η is the dynamic viscosity. f_{water} was measured and the data fit the von Karman equation for water flowing in smooth circular pipes (eq 3) at $Re >$ 10 000. This equation was used for subsequent calculations of f_{water}:

$$\frac{1}{\sqrt{f_{water}}} = 4.0 \log(Re\sqrt{f_{water}}) - 0.4 \qquad (3)$$

The heat loss per unit time in the annulus and heat gain per unit time in the inner tube were measured to ensure they were balanced. The difference was generally less than 5% and was mostly less than 3%. The average of these two quantities was used to calculate heat transfer coefficients. The inlet temperature (T3) was controlled at 10 ± 0.3 °C, and the log-mean temperature difference between the annulus and tube was controlled at 35 ± 0.3 °C. The thermocouple (T4) at the exit of the tube-in-tube heat exchanger was placed at the center of the flow to measure the mean temperature of the fluid. However, this measurement was complicated by a radial temperature gradient established in the fluid, once it got heated by the inner wall of the heat exchanger. Therefore, a helical static mixer was placed just upstream of T4 so that the fluid was well-mixed before reaching that point. Good heat balances could then be obtained under approximately steady-state conditions. The modified Wilson-plot method was used to calculate the heat transfer coefficient and Nusselt number, Nu, of the solution.[20] Nu is the ratio of convective to conductive heat transfer normal to the boundary and is defined as hD/k, where h is the convective heat transfer coefficient and k is thermal conductivity. Heat-transfer reduction (relative to water) was then calculated by eq 4. (Note that low values of % HTR indicate good heat transfer close to that of water.)

$$\% \ HTR = \frac{Nu_{water} - Nu}{Nu_{water}} \times 100\% \qquad (4)$$

where % HTR is percent heat transfer reduction. Nu_{water} is the Nusselt number of water. Nu_{water} and Nu were taken at the same solvent Re.

Experimental results for Nu vs Re for water at 10 °C and $Re > 10 000$ are in good agreement with the Dittus−Boelter equation (eq 5) for water heated in a smooth tube.[57]

$$Nu = 0.023 \ Re^{0.8} \ Pr^{0.4} \qquad (5)$$

where Pr is the Prandtl number, defined as the ratio of viscous diffusion rate to thermal diffusion rate.

2.4. Rheological Measurements. An ARES rheometer (TA Instruments) was used to measure the first normal stress difference (N_1) and shear viscosity of the micellar solutions as functions of shear-rate. A 50 mm cone-and-plate geometry with a cone angle of 0.02 rad was used to measure N_1 vs shear-rate at different temperatures. The measured N_1 readings were corrected for inertial effects according to the following relation:[58]

$$N_1^{corrected} = N_1^{measured} + 0.15\rho\omega^2 R^2 \qquad (6)$$

where ρ is the density of the solution, ω the angular velocity, and R the radius of the cone.

2.5. UV−Visible Spectroscopy and UV Irradiation. UV irradiation of samples was conducted with a 100 W Black-Ray long-wave UV lamp, which emits a broad range of UV radiation centered around the wavelength of 365 nm. For UV−vis spectroscopy and rheological measurements, 10 mL of a given solution was placed in a Petri dish and irradiated for specific durations. For drag reduction and heat transfer experiments, 12 L of solution was divided into 24 portions of 500 mL each. Each portion was held in a beaker and was irradiated by UV under stirring for 30 min. UV−vis spectra were collected on a Hewlett-Packard 8452A diode array spectro-photometer after dilution to 0.04 mM EO12 and 0.05 mM OMCA.

2.6. Cryo-TEM. Cryo-TEM studies on selected samples were carried out at the Technion-Israel Institute of Technology. Cryo-TEM sample preparation was carried out in a controlled environment vitrification system at 100% relative humidity at desired temperatures. A small drop of the studied solution was applied on a perforated carbon film supported on a copper electron microscope grid and then blotted by filter paper into thin films about 10−30 nm thick. The grid was then plunged quickly into liquid ethane near its freezing point (∼90 K) to vitrify the liquid and avoid crystallization. It was then transferred to the cryo-holder of the TEM (FEI T12, operating at 120 kV).[14] Images were taken by a Gatan US1000 cooled CCD camera using the low-dose imaging mode to minimize electron-beam radiation damage.

3. RESULTS AND DISCUSSION

We prepared mixtures of EO12 and OMCA and studied their response using UV−vis spectroscopy, rheometer, and cryo-TEM.

3.1. UV−Visible Spectra. To verify the photoisomerization of *trans*-OMCA to *cis*-OMCA by UV irradiation, UV−vis spectra (Figure 1) were determined for a solution of 0.04 mM EO12 + 0.05 mM *trans*-OMCA, after different durations of UV irradiation, and also for 0.05 mM *cis*-OMCA without irradiation. For wavelengths higher than 220 nm, *cis*-OMCA had two peaks at 256 and 294 nm, while *trans*-OMCA had two peaks at 270 and 310 nm. The
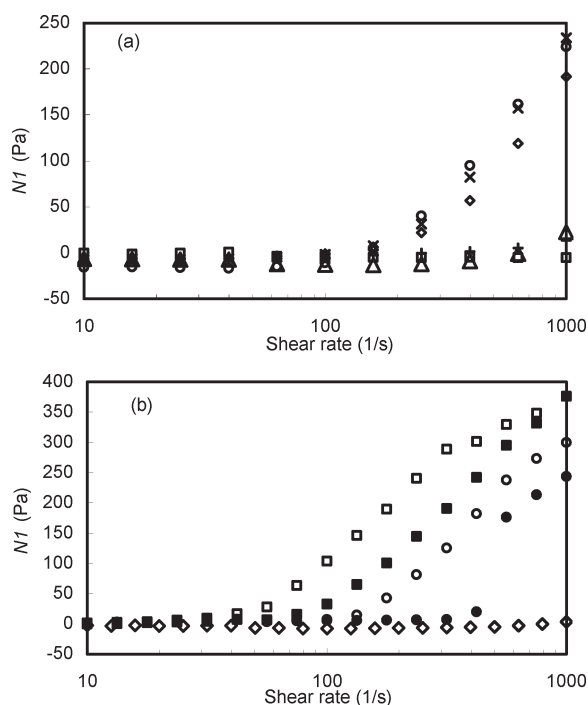
Figure 2. UV effect on N_1 for EO12/*trans*-OMCA solutions of different concentrations at (a) 25 °C (Δ, 4 mM/5 mM; $\square$, 4 mM/5 mM + UV 5 min; $\bigcirc$, 4 mM/8 mM; $\times$, 4 mM/8 mM + UV 100 s; $\diamondsuit$, 4 mM/8 mM + UV 200 s; +, 4 mM/8 mM + UV 300 s) and (b) 10 °C ($\bigcirc$, 4 mM/5 mM; $\bullet$, 4 mM/5 mM + UV 5 min; $\square$, 4 mM/8 mM; $\blacksquare$, 4 mM/8 mM + UV 5 min; $\diamondsuit$, 4 mM/8 mM + UV 10 min). The erratic data for 4 mM EO12 + 8 mM *trans*-OMCA at shear rates greater than 316 s^{-1} were due to the imperfect shape of the sample between the cone and the plate at high rotational speed.

two absorbance peaks of *trans*-OMCA were significantly higher than those of *cis*-OMCA. However, after the sample was irradiated by UV for 1 min, the two peaks of *trans*-OMCA shifted toward a lower wavelength and were lower in magnitude. As the UV irradiation time increased, the two absorbance peaks shifted gradually to those of *cis*-OMCA, and their magnitudes also decreased to the levels of those peaks of *cis*-OMCA after 4 min. The presence of EO12 in the sample had no effect on the spectra of *trans*-OMCA or *cis*-OMCA (data not shown). The shift of absorbance peaks indicated that *trans*-OMCA isomerized to *cis*-OMCA by UV irradiation. The spectra we obtained are nearly identical to those reported previously by Ketner et al.[54] We also irradiated a 4 mM EO12 + 5 mM *trans*-OMCA solution sample, then diluted it to 0.04 mM/0.05 mM, and performed spectrophotometric measurement on it. The latter required longer exposure time (15 min) to reach essentially the same spectra showing that the photoisomerization can take place inside the giant micelles.

For further studies, we chose sample compositions based on our previous experience with EO12-based drag-reducing fluids. Specifically, we chose a low concentration (4 mM) of EO12; this is to ensure that the sample viscosity remains quite low (i.e., comparable to water), which is an important consideration for DR systems. We then added an equimolar or higher amount of OMCA to the EO12 sample to induce growth of threadlike micelles.

3.2. Rheology. The effects of UV irradiation on the rheology of EO12/*trans*-OMCA samples were investigated with respect to the first-normal stress difference, N_1, and the shear viscosity.
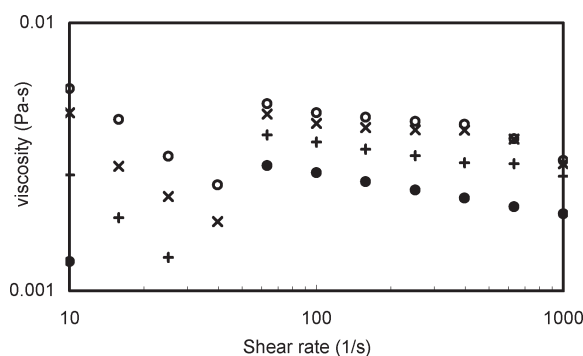

Figure 3. UV effect on shear viscosity of 4 mM EO12 + 8 mM *trans*-OMCA at 25 °C ($\bigcirc$, 0 s; $\times$, 100 s; +, 200 s; $\bullet$, 300 s).

From earlier work, we know that for many DR solutions, a large value of N_1 at high shear-rates correlates with effective drag reduction.[59] Figure 2a shows N_1 data at 25 °C for 4 mM EO12 solutions containing 5 and 8 mM *trans*-OMCA, respectively.

In the case of the 8 mM *trans*-OMCA sample, N_1 increased to ~220 Pa at 1000 s^{-1}. There was little decrease of N_1 after UV irradiation of 100 and 200 s, but after 300 s of UV irradiation, N_1 was reduced to much lower values, only ~10 Pa at 1000 s^{-1}. The other sample, which had a lower *trans*-OMCA concentration of 5 mM showed lower N_1 values: (~20 Pa) even at 1000 s^{-1}. After 300 s of UV irradiation, the N_1 of this sample was reduced to essentially zero.

Data on N_1 were also obtained on the above samples at 10 °C (Figure 2b), which is in the range of the fluid temperatures (~5−15 °C) used in district cooling systems. For the 8 mM *trans*-OMCA solution, Figure 2b shows that the N_1 values were high before UV irradiation. In fact, the sample was so viscoelastic that the high rotational rate of the plate destroyed the shape of the sample resulting in erratic data at shear rates greater than 316 s^{-1}. At shear rates above 40 s^{-1}, reduction of N_1 by 5 min of UV irradiation was observed. After 10 min of irradiation, N_1 values are essentially zero at all shear rates. For the 5 mM *trans*-OMCA solution, Figure 2b shows that the N_1 values at high shear-rates were quite high before UV (~300 Pa at 1000 s^{-1}). UV irradiation for 300 s reduced N_1 across the range of shear-rates, and it was reduced to ~240 Pa at 1000 s^{-1}.

We also tried to measure the viscosity of the above solutions at 25 °C. For the 8 mM *trans*-OMCA sample, the viscosity in Figure 3 shows modest shear-thickening behavior up to a peak at ~80 s^{-1} followed by shear-thinning. Such a response, often termed shear-induced structuring (SIS), is typical of threadlike micellar solutions at these low surfactant concentrations. Similar results were reported by other researchers.[11,60−64] Also, we note that UV irradiation reduces the viscosity across the range of shear-rates. For the 5 mM *trans*-OMCA sample, the viscosity was too low to be measured accurately by our rheometer.

Together the above data show that UV irradiation of EO12/*trans*-OMCA samples for 300 s causes a drop in their viscosity (Figure 3) as well as their viscoelasticity in terms of N_1 (Figure 2). These results are consistent with the findings of Ketner et al.,[54] which were acquired with a different cationic surfactant (CTAB) and at higher concentrations of the surfactant and the *trans*-OMCA. The reductions in rheological properties are expected to be reflected in the nanostructure before and after UV irradiation, i.e., the threadlike micelles are expected to be shortened by UV.

3.3. Cryo-TEM. To obtain direct evidence for UV-induced nanostructural changes, we turned to cryo-TEM. Cryo-TEM images before and after 300 s of UV irradiation are shown in
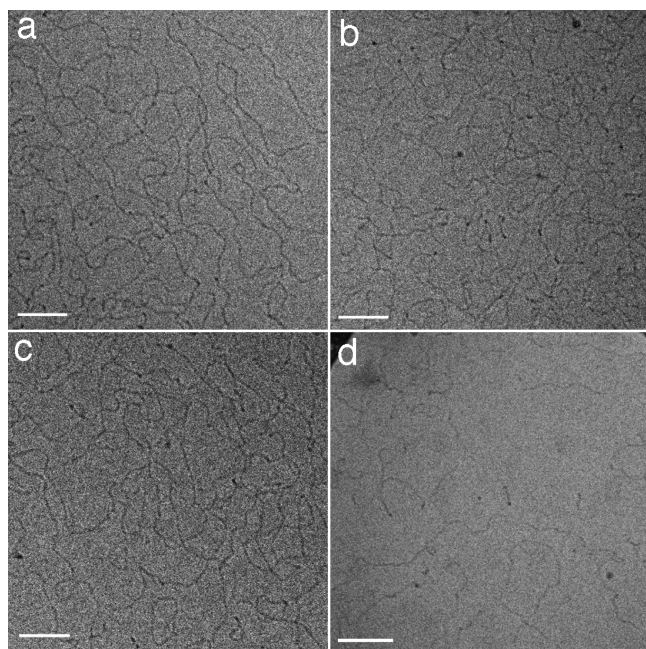
Figure 4. Cryo-TEM images of (a) 4 mM EO12 + 8 mM *trans*-OMCA before UV irradiation, (b) 4 mM EO12 + 8 mM *trans*-OMCA after UV irradiation, (c) 4 mM EO12 + 5 mM *trans*-OMCA before UV irradiation, and (d) 4 mM EO12 + 5 mM *trans*-OMCA after UV irradiation. All scale bars correspond to 100 nm.
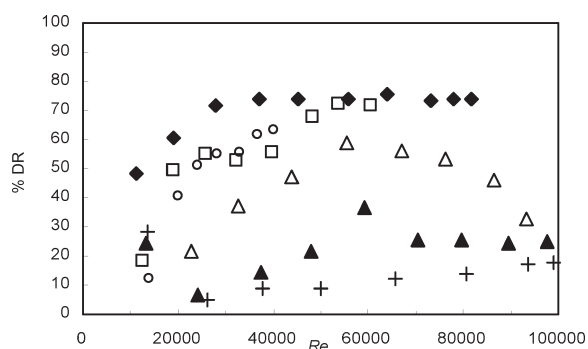

Figure 5. Drag reduction vs Reynolds number for aqueous solution of 4 mM EO12 + 8 mM *trans*-OMCA at different temperatures (○, 5 °C; □, 15 °C; ◆, 30 °C; △, 40 °C; ▲, 45 °C; +, 50 °C).

Figure 4. Before UV, both samples (Figure 4a,c) reveal numerous long threadlike micelles. The cryo-TEM image of the 8 mM *trans*-OMCA sample after UV (Figure 4b) shows reduction in the density of threadlike micelles, but there is no discernible difference in micellar lengths. In comparison, the 5 mM *trans*-OMCA sample after UV (Figure 4d) showed only a few small threadlike micelles, i.e., the sizes of the micelles were considerably smaller than those present before UV and are similar to those present in a 4 mM EO12 + 5 mM *cis*-OMCA sample where no threadlike micelles were observed (cryo-TEM image, not shown). Thus, the expected reduction in micellar sizes due to UV irradiation is clearly seen in the case of the 5 mM *trans*-OMCA sample, while such a reduction is not readily apparent in the case of the 8 mM *trans*-OMCA sample with its higher *trans*-OMCA content.

3.4. Drag Reduction and Heat Transfer Properties. Drag reduction data for the 4 mM EO12 + 8 mM *trans*-OMCA sample
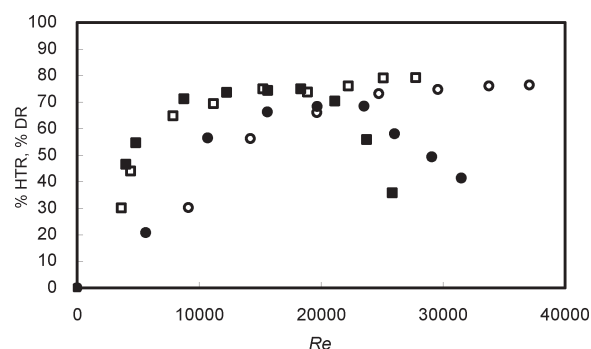

Figure 6. Drag reduction and heat transfer reduction vs Reynolds number for aqueous solution of 4 mM EO12 + 8 mM *trans*-OMCA at 10 °C before and after UV irradiation (○, % DR before UV; □, % HTR before UV; ●, % DR after 30 min of UV irradiation; ■, % HTR after 30 min of UV irradiation).

at temperatures between 5 and 50 °C are shown in Figure 5. In such experiments, a percent drag reduction (% DR) of 50% or higher is a standard cutoff to demarcate drag reducing additives which are effective and potentially useful in applications.[65] On the basis of this cutoff, the above solution is drag-reducing between 5 and 40 °C but not at higher temperatures. At 5 °C, % DR reaches about 60% at a *Re* of 40 000 (higher *Re* values could not be attained at this temperature because of the high viscosity of the solution). From 15 to 30 °C, % DR levels off at about 70% at high *Re*. Finally, at 40 °C, the % DR peaks just above 50% at a *Re* of 55 000 and decreases as the *Re* is increased further. The loss of DR at high temperatures is because the length of threadlike micelles drops with temperature.[65] In summary, the data show that this EO12/*trans*-OMCA solution is drag-reducing at low temperatures and thus might be a candidate for use in district cooling systems.

Figure 6 shows the drag reduction and heat-transfer properties of the above 4 mM EO12 + 8 mM *trans*-OMCA solution at 10 °C, before and after UV irradiation. Before UV, the % DR reaches about 75% at the highest *Re* (about 37 000). After UV irradiation, % DR peaks at about 68% at a *Re* of 23 000 and then decreases to 41% at a *Re* of 32 000. On the basis of the maximum % DR at a *Re* of 23 000, we calculate a critical value of the wall shear stress of 8.9 Pa for the irradiated sample compared with >14.9 Pa, which is the highest value we could measure for the fresh solution. The drag reducing effective *trans*-OMCA concentration has been depleted by radiation to form nondrag reducing *cis*-OMCA. The lower concentration of *trans*-OMCA solution is sensitive to shear degradation and thus is less effective in drag reduction compared to the initial sample.

Next, we consider the percent heat transfer reduction (% HTR). Before UV, the % HTR increased to nearly 80% at high *Re*, indicating very poor heat transfer. After UV irradiation, the % HTR was about the same at *Re* below 18 000 but decreased sharply at higher *Re*. Thus, UV irradiation improves the heat transfer properties of this solution at high *Re* but not at low *Re*, which tracks roughly (in the opposite direction) the diminished drag reduction behavior. Aguilar et al.[33] noted that % HTR was always greater than % DR, as also observed here.

Similar data for the 4 mM EO12 + 5 mM *trans*-OMCA sample at temperatures between 1 and 40 °C are shown in Figure 7. The solution is drag reducing (% DR > 50%) from 1 to 30 °C. The % DR reaches about 70% at intermediate values of *Re* and
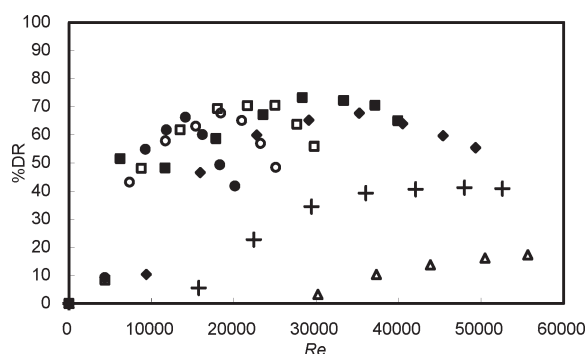
Figure 7. Drag reduction vs Reynolds number for aqueous solution of 4 mM EO12 + 5 mM *trans*-OMCA at different temperatures (●, 1 °C; ○, 5 °C; □, 10 °C; ■, 20 °C; ◆, 30 °C; +, 35 °C; △, 40 °C).
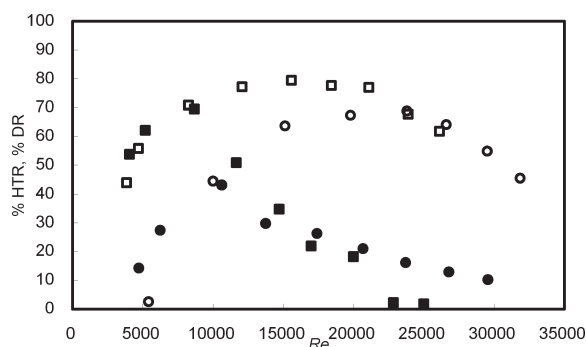

Figure 8. Drag reduction and heat transfer reduction vs Reynolds number for aqueous solution of 4 mM EO12 + 5 mM *trans*-OMCA at 10 °C before and after UV irradiation (○, % DR before UV; □, % HTR before UV; ●, % DR after 30 min of UV irradiation; ■, % HTR after 30 min of UV irradiation).

then decreases with a further increase in Re. The % DR at high Re values is somewhat lower for this sample than for the 8 mM *trans*-OMCA sample (Figures 7 and 8), indicating that the micelles in this solution are not as effective drag-reducers, but this system is still a good candidate for district cooling.

Figure 8 shows % DR and % HTR at 10 °C vs Reynolds number for this solution, before and after UV irradiation. Before UV, the % DR increases to 67% at a Re of 24 000 and then decreases to 42% at a Re of 31 500. After UV irradiation, the highest % DR is only 43% at a Re of ~10 000, which is below the 50% threshold for drag reduction, i.e., this solution cannot be considered an effective drag-reducer. Turning now to the % HTR, we see that before UV, the % HTR increases to nearly 79% at a Re of 16 000 and then decreases to 61% at a Re of 26 000. However, after UV irradiation, the heat transfer was improved significantly, that is, the % HTR values are much lower for the irradiated sample and, in fact, the % HTR drops to nearly zero at $Re > 22 000$. That is, at high Re, the irradiated sample shows enhanced heat transfer, similar to that of water, reflecting the diminished sizes of the threadlike micelles.

The effects on Nusselt numbers (Nu) of this 4 mM EO12 + 5 mM *trans*-OMCA sample compared to those of water are shown in Figure 9. The Nu values of the solution before UV increase with Re but are well below those of water. After UV irradiation for 30 min, the solution shows significantly higher Nu values, which approach those of water at $Re \sim 25 000$. Again,
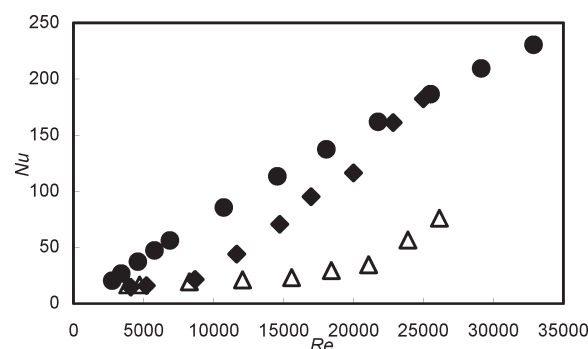

Figure 9. Nusselt number vs Reynolds number of 4 mM EO12 + 5 mM *trans*-OMCA solution before and after UV irradiation (●, water; ◆, solution after UV; △, solution).

these results indicate the enhanced heat-transfer properties of the irradiated sample.

With these encouraging results for enhancing heat transfer, we now plan to find conditions to reverse the isomerization of the photosensitive OMCA counterion, back from cis to trans. As shown by Scheme S1 in the Supporting Information, we could then subject the drag reducing solution to irradiation to isomerize OMCA from trans to cis at the entrance to the heat exchanger (thus converting long micelles to short ones) and thereafter irradiation to isomerize OMCA from cis to trans at the exit from the heat exchanger (restoring the long micelles and thereby the DR properties).

4. CONCLUSIONS

UV irradiation of EO12/*trans*-OMCA results in isomerization of much of the trans to cis configuration, as confirmed by UV−vis spectra. In turn, this causes a reduction in micelle size, as shown by cryo-TEM images for 4 mM EO12 + 5 mM *trans*-OMCA solution. That leads to significant reduction in viscosity and viscoelasticity of the solution. The drag reducing character of the solution is thereby lowered and its heat-transfer properties are substantially enhanced. Our study shows that the use of photosensitive micelles is a promising approach to developing effective drag reducing systems for use in district cooling and district heating systems.

■ ASSOCIATED CONTENT

ⓢ Supporting Information. Details of the recirculation system as well as structures of OMCA are shown. This material is available free of charge via the Internet at http://pubs.acs.org.

■ AUTHOR INFORMATION

Corresponding Author
*E-mail: zakin.1@osu.edu.

Present Addresses
⊗Research Center of Chemical Engineering, East China University of Science and Technology, 130 Meilong Road, Shanghai 200237, China.

■ ACKNOWLEDGMENT

■ REFERENCES

(1) Forrest, F.; Grierson, G. A. H. *Pap. Trade J.* **1931**, *22*, 39–41.

(2) Nadolink, R. H.; Haigh, W. W. *Appl. Mech. Rev.* **1995**, *48*, 351–460.

(3) Virk, P. S. *J. Appl. Mech.* **1970**, *37*, 488–493.

(4) Zakin, J. L.; Myska, J.; Chara, Z. *AIChE J.* **1996**, *42*, 3544–3546.

(5) Poggi, Y. *J. Phys. Chem.* **1984**, *88*, 5713–5720.

(6) Kumar, S.; Naqvi, A. Z.; Kabir-ud-Din *Langmuir* **2000**, *16*, 5252–5256.

(7) Lu, B. *Characterization of Drag Reducing Surfactant Systems Rheology and Flow Birefringence Measurements*. Ph.D. Dissertation, The Ohio State University, Columbus, OH, 1997.

(8) Lu, B.; Li, X.; Scriven, L. E.; Davis, H. T.; Talmon, Y.; Zakin, J. L. *Langmuir* **1998**, *14*, 8–16.

(9) Lu, B.; Zheng, Y.; Davis, H. T.; Scriven, L. E.; Talmon, Y.; Zakin, J. L. *Rheol. Acta* **1998**, *37*, 528–548.

(10) Lin, Z.; Chou, L.; Lu, B.; Zheng, Y.; Davis, H. T.; Scriven, L. E.; Talmon, Y.; Zakin, J. L. *Rheol. Acta* **2000**, *39*, 0354–0359.

(11) Lin, Z.; Lu, B.; Zakin, J. L.; Talmon, Y.; Zheng, Y.; Davis, H. T.; Scriven, L. E. *J. Colloid Interface Sci.* **2001**, *239*, 543–554.

(12) Lin, Z.; Mateo, A.; Zheng, Y.; Kesselman, E.; Pancallo, E.; Hart, D. J.; Talmon, Y.; Davis, H. T.; Scriven, L. E.; Zakin, J. L. *Rheol. Acta* **2002**, *41*, 483–492.

(13) Zhang, Y.; Schmidt, J.; Talmon, Y.; Zakin, J. L. *J. Colloid Interface Sci.* **2005**, *286*, 696–709.

(14) Talmon, Y. *Seeing Giant Micelles by Cryogenic-Temperature Transmission Electron Microscopy (Cryo-TEM)*; Zana, R., Kaler, E. W., Eds.; Surfactant Science Series 140; CRC Press: New York, 2007; pp 163−178.

(15) Ge, W.; Kesselman, E.; Talmon, Y.; Hart, D. J.; Zakin, J. L. *J. Non-Newtonian Fluid Mech.* **2008**, *154*, 1–12.

(16) Ohlendorf, D.; Interthal, W.; Hoffmann, H. *Rheol. Acta* **1986**, *25*, 468–486.

(17) Rehage, H.; Wunderlich, I.; Hoffmann, H. *Prog. Colloid Polym. Sci.* **1986**, *72*, 51–59.

(18) Bewersdorff, H. W. *Colloid* **1988**, *266*, 941.

(19) Zakin, J. L.; Lu, B.; Bewersdorff, H. *Rev. Chem. Eng.* **1998**, *14*, 253.

(20) Qi, Y. *Investigation of Relationships among Microstructure, Rheology, Drag Reduction and Heat Transfer of Drag Reducing Surfactant Solutions*. Ph.D. Dissertation, The Ohio State University, Columbus, OH, 2002.

(21) Gyr, A.; Bühler, J. *J. Non-Newtonian Fluid Mech.* **2010**, *165*, 672–675.

(22) Tamano, S.; Itoh, M.; Inoue, T.; Kato, K.; Yokota, K. *Phys. Fluids* **2009**, *21*, 045101–045119.

(23) Anacker, E. *J. Phys. Chem.* **1984**, *88*, 2390–2393.

(24) Lin, Z. *The Effect of Chemical Structures of Cationic Surfactants or Counterions on Solution Drag Reduction Effectiveness, Rheology and Micellar Microstructure*. Ph.D. Dissertation, The Ohio State University, Columbus, OH, 2000.

(25) Smith, B. C.; Chou, L. C.; Zakin, J. L. *J. Rheol.* **1994**, *38*, 73–83.

(26) Lin, Z.; Zakin, J. L.; Zheng, Y.; Davis, H. T.; Scriven, L. E.; Talmon, Y. *J. Rheol.* **2001**, *45*, 963–981.

(27) White, A. *Nature* **1970**, *227*, 486–487.

(28) Monti, R. *Progr. Heat Mass Transfer* **1972**, *S*, 239–261.

(29) Debrule, P. M.; Sabersky, R. H. *Int. J. Heat Mass Transfer* **1974**, *17*, 529–540.

(30) Dimant, Y.; Poreh, M. *Adv. Heat Transfer* **1976**, *12*, 77–113.

(31) Matthys, E. F. *J. Non-Newtonian Fluid Mech.* **1991**, *38*, 313–342.

(32) Aguilar, G.; Gasljevic, K.; Matthys, E. F. *Am. Soc. Mech. Eng.* **1998**, *361−1*, 139–146.

(33) Aguilar, G.; Gasljevic, K.; Matthys, E. F. *Int. J. Heat Mass Transfer* **2001**, *44*, 2835–2843.

(34) Sellin, R. H. J.; Hoyt, J. W.; Scrivener, O. *J. Hydraulic Res.* **1982**, *20*, 29.

(35) Myska, J.; Zakin, J. L.; Chara, Z. *Appl. Sci. Res.* **1995**, *55*, 297–310.

(36) Tamano, S.; Itoh, M.; Kato, K.; Yokota, K. *Phys. Fluids* **2010**, *22*, 055102–055112.

(37) Kawaguchi, Y.; Segawa, T.; Feng, Z.; Li, P. *Int. J. Heat Fluid Flow* **2002**, *23*, 700–709.

(38) Li, F.; Kawaguchi, Y.; Yu, B.; Wei, J.; Hishida, K. *Int. J. Heat Mass Transfer* **2008**, *51*, 835–843.

(39) Qi, Y.; Kawaguchi, Y.; Lin, Z.; Ewing, M.; Christensen, R. N.; Zakin, J. L. *Int. J. Heat Mass Transfer* **2001**, *44*, 1495–1505.

(40) Li, P.; Kawaguchi, Y.; Daisaka, H.; Yabe, A.; Hishida, K.; Maeda, M. *J. Heat Transfer* **2001**, *123*, 779–789.

(41) Qi, Y.; Kawaguchi, Y.; Christensen, R. N.; Zakin, J. L. *Int. J. Heat Mass Transfer* **2003**, *46*, 5161–5173.

(42) Wang, D.; Dong, Z. Method for controlling turbulent flow and heat conduction character of drag reduction fluid. C.N. Patent 1603637, April 6, 2005.

(43) Aly, W. I. A.; Inaba, H.; Haruki, N.; Horibe, A. *J. Heat Transfer* **2006**, *128*, 800–810.

(44) Zhou, T.; Leong, K. C.; Yeo, K. H. *Int. J. Heat Mass Transfer* **2006**, *49*, 1462–1471.

(45) Mizunuma, H.; Kobayashi, T.; Tominaga, S. *J. Non-Newtonian Fluid Mech.* **2010**, *165*, 292–298.

(46) Qi, Y.; Weavers, L. K.; Zakin, J. L. *J. Non-Newtonian Fluid Mech.* **2003**, *116*, 71–93.

(47) Wolff, T.; Kerperin, K. J. *J. Colloid Interface Sci.* **1993**, *157*, 185–195.

(48) Yu, X.; Wolff, T. *Langmuir* **2003**, *19*, 9672–9679.

(49) Lehnberger, C.; Wolff, T. *J. Colloid Interface Sci.* **1999**, *213*, 187–192.

(50) Moleavin, I.; Grama, S.; Carlescu, I.; Scutaru, D.; Hurduc, N. *Polym. Bull.* **2010**, *65*, 69–81.

(51) Eastoe, J.; Vesperinas, A. *Soft Matter* **2005**, *1*, 338–347.

(52) Hubbard, F. P., Jr.; Abbott, N. L. *Stimuli-Responsive Giant Micellar Systems*; Zana, R., Kaler, E. W., Eds.; Surfactant Science Series 140; CRC Press: New York, 2007; pp 375−395.

(53) Sakai, H.; Orihara, Y.; Kodashima, H.; Matsumura, A.; Ohkubo, T.; Tsuchiya, K.; Abe, M. *J. Am. Chem. Soc.* **2005**, *127*, 13454–13455.

(54) Ketner, A. M.; Kumar, R.; Davies, T. S.; Elder, P. W.; Raghavan, S. R. *J. Am. Chem. Soc.* **2007**, *129*, 1553–1559.

(55) Kumar, R.; Ketner, A. M.; Raghavan, S. R. *Langmuir* **2010**, *26*, 5405–5411.

(56) Ge, W. *Studies on the Nanostructure, Rheology and Drag Reduction Characteristics of Drag Reducing Cationic Surfactant Solutions*. Ph.D. Dissertation, The Ohio State University, Columbus, OH, 2008.

(57) Shi, H.; Wang, Y.; Fang, B.; Huggins, J. T.; Huber, T. R.; Zakin, J. L. *Adv. Mech. Eng.*, Special Issue: Drag Reduction of Turbulent Flow by Additives, accepted.

(58) Macosko, C. W. *Rheology: Principles, Measurements, and Applications*; Wiley-VCH: New York, 1994.

(59) Qi, Y.; Littrell, K.; Thiyagarajan, P.; Talmon, Y.; Schmidt, J.; Lin, Z.; Zakin, J. L. *J. Colloid Interface Sci.* **2009**, *337*, 218–226.

(60) Wunderlich, I.; Hoffmann, H.; Rehage, H. *Rheol. Acta* **1987**, *26*, 532–542.

(61) Wunderlich, A. M.; Brunn, P. O. *Colloid Polym. Sci.* **1989**, *267*, 627–636.

(62) Liu, C.; Pine, D. J. *Phys. Rev. Lett.* **1996**, *77*, 2121–2124.

(63) Hu, Y.; Matthys, E. F. *J. Rheol.* **1997**, *41*, 151–166.

(64) Oda, R.; Narayanan, J.; Hassan, P. A.; Manohar, C.; Salkar, R. A.; Kern, F.; Candau, S. J. *Langmuir* **1998**, *14*, 4364–4372.

(65) Chou, L. C. *Drag-reducing cationic surfactant solutions for district heating and cooling systems*. Ph.D. Dissertation, The Ohio State University, Columbus, OH, 1991.
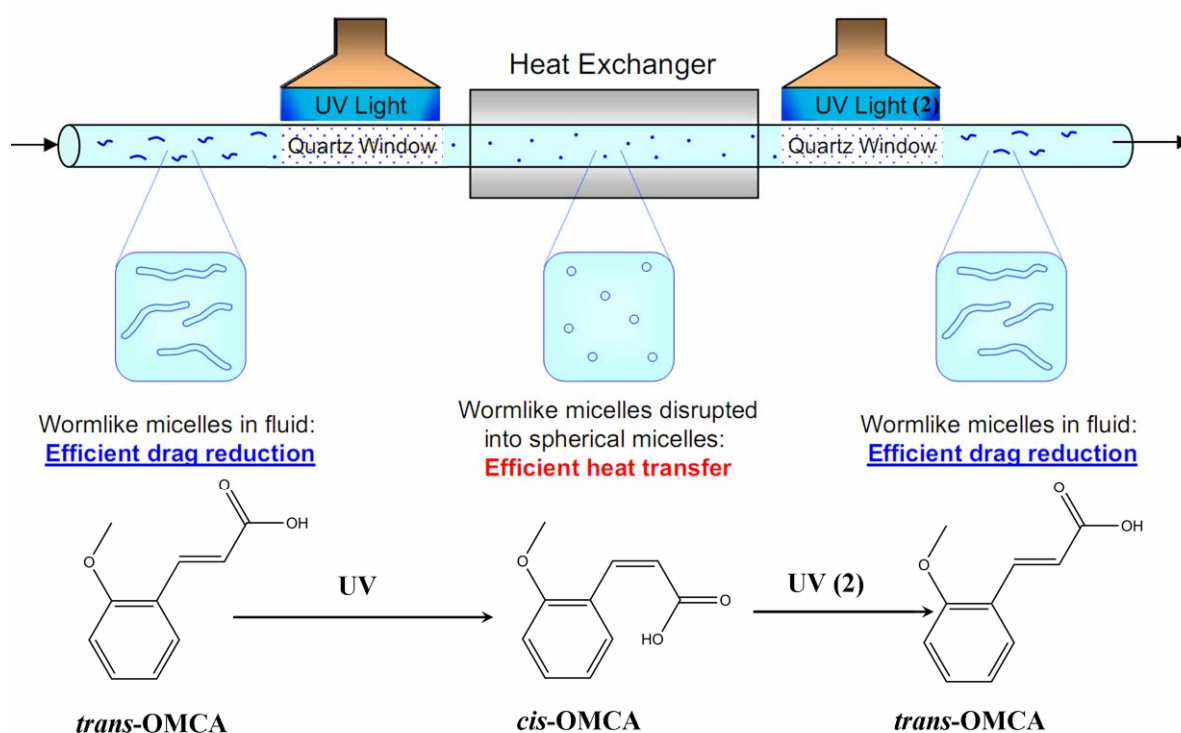
Supporting Information

Light-Responsive Threadlike Micelles as Drag Reducing Fluids with Enhanced Heat-Transfer Capabilities

Haifeng Shi, Yi Wang, Bo Fang, Yeshayahu Talmon, Wu Ge, Srinivasa R. Raghavan,

Jacques L. Zakin

Scheme S1. The use of light-responsive fluids to ensure both efficient drag reduction

in pipe flow as well as efficient heat transfer in the heat exchanger.

Description of the Recirculation System.

A schematic of our recirculation system for drag reduction and heat-transfer experiments is shown in Scheme S2. The system consists of a reservoir tank, a pump, two heat exchangers, an electric heater, a chiller, two circulators, a magnetic flow meter (TOSHIBA LF404), a number of T-type thermocouples, and a series of pressure transmitters (OMEGA PX2300 series). The shell side of the tube-in-tube heat exchanger has two circulators (NESLAB RTE-111 and VWR 1160) connected in series, while the shell side of the fluted tube-in-tube heat exchanger is connected to a chiller (Bay Voltex). All the tubes, pipes and heat exchangers are insulated with Nomaco K-Flex polyolefin to minimize heat exchange with the environment. The pumping system consists of a centrifugal pump (PROCON) with a motor controller (BALDOR Adjustable Speed Drive) to regulate the pump rotation in the range of 0 to 1969 rpm. The flow rate (0.04 to 0.35 L/s) is monitored by a flow meter.

An electric heater (TrueHeat 1500W) maintains the main loop temperature from room temperature up to ~ 50ºC. The chiller in the annulus loop of the fluted tube-in-tube heat exchanger (with a coolant of 50% ethylene glycol and 50% water) cools and maintains the temperature of the main loop. The temperature of the shell side of the tube-in-tube heat exchanger is mediated by the circulators and can be varied from 0 to 90 °C. The flow rate in the shell side is preset for each experiment to keep the heat transfer resistance on the shell side constant. Temperatures at all locations are measured by the thermocouples (T1 through T4 and T9 through T12).

Scheme S2. Schematic of apparatus for drag reduction and heat transfer experiments.

The differential pressures of straight pipe sections are measured by the pressure transmitters (P1 through P10). Transmitters P1 through P9 measure consecutive sections of straight pipe. P1 measures the pressure difference across a section of 50 pipe diameters. P2 measures the differential pressure across a pipe section of 180 diameters, including the tube-in-tube heat exchanger. P3 through P9 each measures differential pressures across 80 diameters length downstream of the tube-in-tube heat exchanger.

The recirculation loop has a total length of about 25 m and can hold up to 16 L of liquid. The smooth stainless pipe has an inner diameter (ID) of 10.2 mm and an outer diameter (OD) of 12.7 mm. The reservoir tank has a volume of 14 L. The 0.914 m long tube-in-tube heat exchanger has the same tube diameter. The ID of the outer shell is 50 mm. All heat transfer measurements were taken on the tube-in-tube heat exchanger. All the thermocouples, pressure transmitters and flow meters are connected to the data acquisition system.